UDC 669 . 14 - 427 . 4 : 624 . 5 : 624 . 042 .4

Development of Lowdrag Aerodynamically Stable Cable with Indented Processing

Tetsuo HOJO*1 Shinsuke YAMAZAKI*1
Hiroyuki OKADA*1

Abstract

A wind-resistant design of cables for large cable-stayed bridges is required as a measure against rain-wind induced vibration. In such bridges, many cables are arranged in a short pitch, which causes a large drag force on the cables. Therefore, reduction of drag force on cables is essential for rationalizing bridge design, as well as restraint of vibration. This paper describes studies on a new cable having both a low drag co-efficient force and rain-vibration suppressing effects. Through many investigations using wind tunnel tests, an indented cable was developed as a countermeasure against rain-wind induced vibration, and finally it was applied to the Tatara Bridge which is the largest cable-stayed bridge in the world.

1. Introduction

With increased number of cable-stayed bridges, many cases have been reported[1,2] of cable vibration caused by wind. Latest long cable-stayed bridges widely employ single-strand cables with protective coating of polyethylene or the like. Smooth-surfaced cables, however, are often subject to a vibration phenomenon caused by a combination of rain and wind (rain vibration). Various studies have been made in relation to the rain vibration phenomenon and its countermeasures[2,3]. The longer the cable-stayed bridges, the longer the cables employed therein [and], hence, vibration suppression by means of cable fixtures sometimes does not work as expected due to restrictions to the position and structure of the fixtures. In such a context, aerodynamic vibration control measures to make the cables capable by themselves of suppressing vibration are becoming more and more important.

Besides, since many cables are arranged close to each other in long cable-stayed bridges, the wind load on them account for a large proportion of the total wind load on the entire bridge. Hence, it is essential to minimize the wind load on the cables for rationalizing design of the bridges. Aerodynamic cable section shapes so far proposed for vibration control envisaged forming of cable surfaces so as to obtain rain vibration suppression effects, but overall aerodynamic cable characteristics including factors such as drag coefficient have little been studied.

The present paper aims at studying vibration control measures of the cables focusing on the above issue and describes development of a vibration suppressing cable characterized by being aerodynamically stable against the rain vibration and having a small drag coefficient.

2. Technical Problems of Cables for Long Cable-stayed Bridges

2.1 Reduction of Wind Loads on Cables

Many of the latest long cable-stayed bridges are composed of multiple cables and slender box girders, and wind load on the cables tend to account for an increasingly greater proportion in the total wind load of the bridge. **Fig.1** shows a comparison of the relationship of the wind load on the cables and the same on the girder, calculated on an assumption that the structural components are of a 1,000-m class cable-stayed bridge. The longer the cable-stayed bridges are the larger the wind load on the cables becomes, and it tends to become larger than the wind load on the girder. In this process, the drag coefficient of the cables tends to bring about more and more direct

*1 Civil Engineering & Marine Construction Division

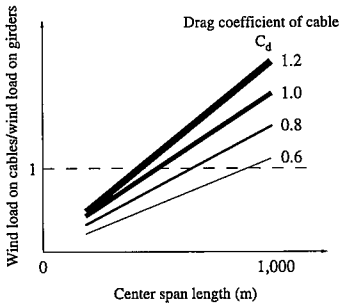

Fig.1 Wind loads on cables and girders of cable-stayed bridge

effects on the wind load. When their drag coefficient is increased, it will influence on sectional design of the other members, such as towers and girders, the sections of which are determined in consideration of storms. In this sense it is very important for rational design of long cable-stayed bridges to minimize the wind load on the cables through reduction of their drag coefficient.

Since cables are structural members of a columnar shape, their drag coefficient is largely influenced by Reynolds number Re[4]. (Re = UD/ν, where U is wind velocity, D is diameter, and ν is kinematic viscosity coefficient.) Generally speaking, the critical Reynolds number of a smooth-surfaced infinite column is approximately 4×10^5 with the diameter as a characteristic length and, assuming that the standard cable diameter of long cable-stayed bridges is 15 cm or so, this approximately corresponds to the design wind velocity range. The range of Reynolds number values lower than the critical Reynolds number is called sub-critical range and the range higher than that supercritical range. (See **Fig.2.**) It is understood that the state of peeling of peripheral airflow around a columnar body gradually changes near the critical Reynolds number from the so-called laminar flow peeling to the turbulent flow peeling.

The drag coefficient of a smooth-surfaced column is approximately 1.2 in the sub-critical range, and after dropping to somewhere below 0.5 at the critical Reynolds number it increases in the supercritical range as the state of airflow stabilizes in the state of turbulent flow peeling. In the case of a typical size cable for cable-stayed and suspension bridges having a smooth surface, a drag coefficient value of 0.7 is used in the bridge design, since the design wind velocity falls within the critical Reynolds number range where the drag coefficient falls by a great amount.

Different from the above, in the case of a column having roughness evenly distributed on its surface, it is known that the critical Reynolds number shifts to the lower side and that the drag coefficient increases as the Reynolds number goes up. It is said that when the column surface has deformations about 1% of the diameter large, for example, the critical Reynolds number is about 6×10^4 and the drag coefficient increases to roughly 1 around the design wind velocity. Further, with conventional aerodynamic measures against rain vibration through cable surface treatment, such as, with ridges or groves running in parallel on the surface, the drag coefficient approaches asymptotically to 1.2 in the high Reynolds number range or the design wind velocity range.

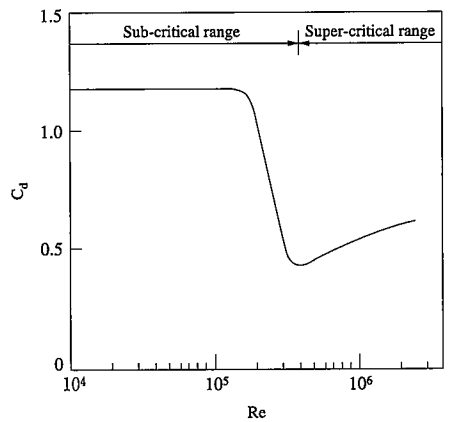

Fig.2 Relationship between drag coefficient and Reynolds number of round section body

As described above, drag coefficient is the minimum when the surface is smooth and it increases as the surface roughness or deformation becomes coarser for enhancing vibration suppression effects. This means that, as far as the conventional measures are concerned, aerodynamic cable stabilizing measures contradict with reduction of drag coefficient, which fact is quite inconvenient for rationalizing the structure of long cable-stayed bridges. It becomes necessary, therefore, to develop a new aerodynamic cable section for improving the drag characteristics and effectively suppressing the rain vibration at the same time.

2.2 Vibration Suppression Measures of Cables

2.2.1 Vibration Phenomena of Cables

Cable length of cable-stayed bridges became very long as bridges grew longer: in the case of a bridge with a 1,000 m center span, for example, the distance between cable anchoring [anchorages] can be as long as 500 m. Besides, since the cable section is basically round and little structural damping can be expected there to be, vibration is easily caused by wind. There are three kinds of vibration phenomena caused by wind to the cables: vortex-induced excitation, rain vibration and wake galloping.

The vortex-induced excitation is a vibration phenomenon appearing when the period of alternate vortex in the wake coincides with the vibration period of the cable. The wind speed that causes the vortex-induced excitation can be calculated from the equation U = fD/S, where f is natural frequency of the cable, D is the cable diameter, and S is Strouhal number. The generation mechanism of the vortex-induced excitation is such that its vibration usually appears as a restricted amplitude oscillation and takes place at a low wind speed range, and amplitude is comparatively small. As its excitation force is weak, it has been confirmed that the vibration can be controlled by addition of damping means such as cushioning materials to the cable anchoring [anchorages].

The rain vibration is another vibration phenomenon caused by wind with rain when the cables become aerodynamically unstable due to rivulets of water formed on the surface. According to a recent study[5], although existence of the rivulets is one of the causes of the rain vibration of cable-stayed bridges, there is airflow along the cable axis on the surface of a slanted cable even without rain and, hence, the cable is intrinsically prone to vibrate. Thus, the rain vibration is thought to result from complex combinations of wind and water flow. The rain vibration was first observed in the Meiko Nishi Bridge (near Nagoya, Japan) and then it was also observed in many other cable-stayed bridges such as Hitsuishi-Iwaguro Bridge, Aratsu Bridge, Tempozan Bridge, and so on. The maximum amplitude can be as large as 5 - 6 times the cable diameter. The following characteristics have been made clear about the rain vibration from observations at existing bridges and wind tunnel tests:

1) Cable shape: The rain vibration takes place with smooth-surfaced round section cables.

2) Frequency: Usually less than 3 Hz.
3) Wind speed: The vibration takes place with a wind 6 m/s or stronger accompanied by rain.
4) Wind direction: The vibration is most likely to take place when the cable is in a so-called normal posture, that is, both the vertical angle of the cable axis to the wind direction and the horizontal angle of the same (corresponding to angles α and β of Fig.10) are 45°.
5) Vibration control measures: The vibration can be mostly controlled by addition of damping apparatuses having a logarithmic decrement of around $\delta = 0.02$.

The wake galloping is a vibration occurring to a cable located downwind to another in parallel, caused by the trailing vortex (wake) of the upwind cable. Its occurrence depends on the gap between cables: it easily occurs when the gap is less than 5D, but a wake-induced flutter is considered to take place with larger gaps.

Although the rain vibration is not as seriously dangerous as to cause destruction of the bridge, it is highly likely to damage the cables and their anchoring [anchorages] and therefore, it is imperative to include its countermeasures in the wind resistance design of long cable-stayed bridges. For this reason, this paper covers studies of rain vibration control measures.

2.2.2 Vibration Control Measures

There are three different types of vibration control measures for the cables of cable-stayed bridges[6,7].

Addition of damping apparatuses is a method whereby vibration is suppressed by dampers provided between the cables and the girder for increasing structural damping capacity of the cables, and is a considerably popular practice as a countermeasure against rain vibration. Vibration damping effects of the damper addition can be theoretically calculated pretty accurately. Among various types of dampers, hydraulic dampers (see **Photo 1**), viscous shearing dampers and high damping rubber dampers have been applied to existing bridges. Any of these types can be used for the damper addition method, but it is always necessary to keep watching deterioration of the dampers during the service life and their durability. It has to be noted, however, that in long cable-stayed bridges the dampers have to be installed pretty high above the girder level for obtaining good damping effects. For this reason there may be cases where results are dissatisfactory due to restrictions in the damper location and insufficient rigidity of the damper mounting structure.

The cable interconnection method (see **Fig.3**) is a method for

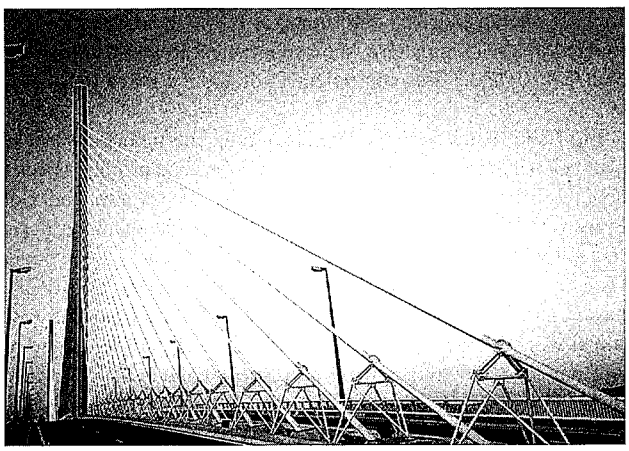

Photo 1 Vibration suppression measure by damper addition (Brotonne Bridge)

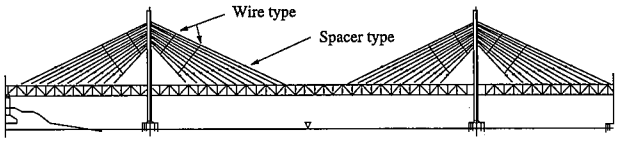

Fig.3 Vibration suppression measures by cable interconnection (Hitsuishi-Iwaguro Bridge)

mechanically restricting vibrations by interconnecting adjacent cables with wires. This method is effective only for vibrations the antinodes of which fall at the connection points and not effective when the vibration nodes coincide with the connection points. It is therefore necessary to select the connection points in consideration of higher-order mode shapes required for vibration suppression. Further, the cable interconnection method requires a thorough preliminary study, since it is not easy to quantitatively predict the damping effects before installation and, in addition, maintenance of connecting wires and jigs has to be given due considerations. Regarding long cable-stayed bridges, when trying to cope with multiform higher-order mode vibrations occurring to long cables, a great number of connecting wires would be required and it would not be realistic to plan to control every possible mode.

Different from the above, aerodynamic measures[8] envisage controlling the very excitation force through forming of cable surfaces. They have, therefore, the advantage of not requiring any cable accessories such as the damper addition, connecting wires, etc. Various cable section shapes have been proposed as aerodynamic measures based on wind tunnel tests, and all of them intend to obtain vibration suppression effects either through prevention of rivulets – a main cause of the rain vibration – from forming or disturbing airflow around the cables. The section shapes actually applied so far to real bridges include parallel ridges[9] (see **Fig.4**), U stripes[10] and helical strakes[11] and their effectiveness is now being confirmed. As described in 2.1, however, these measures increase the drag coefficient of the cables and result in a greatly increased wind load at the design wind velocity range. If the drag coefficient can be lowered, therefore, the aerodynamic measures offer a very promising solution for suppressing cable vibration of long cable-stayed bridges.

From this viewpoint, the authors proceeded to develop countermeasures against rain vibration focusing on the aerodynamic measures. The basic idea of the present study for minimizing the drag coefficient is to extend the drag coefficient characteristics near the critical Reynolds number to higher Reynolds number ranges as well, namely, to work out a cable surface form with which the drag coefficient characteristics near the critical Reynolds number are maintained in a wider range by means of keeping smooth surface portions and

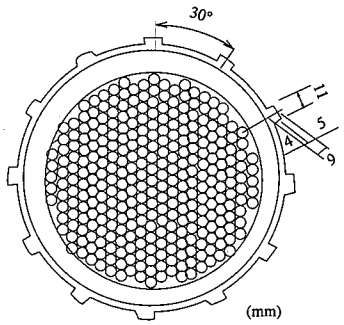

Fig.4 Aerodynamic vibration suppression measures (Higashi Kobe Bridge)

combining them with rough surface portions where turbulent flow peeling occurs easily. Because water rivulets on the cable surface are viewed to have a large influence on the occurrence of rain vibration, it is intended that the vibration is controlled by hindering formation of the rivulets through regulating the airflow around the cable by properly distributing rough portions on the cable surface. For this end, the authors began with studying static aerodynamic properties of cables having rough surface portions.

3. Static Aerodynamic Properties of Cables Having Rough Surface Portions

3.1 Fundamental Tests on Cables Having Rough Surface Portions

For the purpose of understanding influences of surface roughness on static aerodynamic properties of cables, the authors carried out three force component tests[12,13]. Aluminum tubes having diameters equal to real bridge cables were used as models and they were coated with the same polyethylene material used for the real cables and then deformations were formed on the surface. In order for clarifying the influence of surface roughness, three kinds of models having different shapes and distributions of surface roughness were used in the tests. (See **Table 1**.)

An unsteady aerodynamic force wind tunnel (section 2.0 m high and 1.0 m wide) at the Public Works Research Institute of the Ministry of Construction was employed for tests of the models A and B, and the measurements were carried out up to a wind speed of 25 m/s. The maximum Reynolds number obtainable by the wind tunnel is approximately 2.2×10^5. Models C were tested at a large circuit wind tunnel (section 3.0 m high and 2.0 m wide) of Sumitomo Heavy Industries Ltd. at wind tunnel speeds up to 55 m/s (Reynolds number approximately 5.5×10^5), which roughly corresponds to the design wind speed level of real bridges.

As shown in **Fig.5**, the critical Reynolds number of a cable with evenly distributed surface roughness becomes lower as the roughness becomes coarser. It was observed that the larger the relative surface roughness k/D, the larger became the difference by which the value of its drag coefficient at the critical Reynolds number surpasses that of a smooth-surfaced cable ($C_d \fallingdotseq 0.5$), and that the faster the wind the larger tended the drag coefficient, asymptotically approaching 1.2 rapidly. With Model A_6 having evenly distributed surface deformations 1% of the diameter in size, the drag coefficient C_d was roughly 0.9 at a critical Reynolds number of approximately 4×10^4, and C_d was roughly 1.2 at a Re of 2.2×10^5. The tests of the authors covered finer degrees of roughness than past similar tests and the results obtained well conformed to past reports in the roughness coefficient range of 10^{-2} to 10^{-3}.

Table 1 Cable model data

Model	Diameter D (m)	Surface roughness k (μm)	Relative surface roughness (k/D)	Remarks
A_1	0.132	3	2.3×10^{-5}	Smooth surface
A_2	0.122	30	2.5×10^{-4}	Evenly distributed roughness
A_3	0.132	100	7.6×10^{-4}	Evenly distributed roughness
A_4	0.124	200	1.6×10^{-3}	Evenly distributed roughness
A_5	0.124	600	4.8×10^{-3}	Evenly distributed roughness
A_6	0.128	1,500	1.2×10^{-2}	Evenly distributed roughness
B_1	0.147	200	1.4×10^{-3}	Grating pattern
B_2	0.147	600	4.1×10^{-3}	Grating pattern
B_3	0.149	1,200	8.1×10^{-3}	Grating pattern
C_1	0.140	3	2.1×10^{-5}	Smooth surface
C_2	0.140	1,500	1.1×10^{-2}	Discrete depressions
C_3	0.140	1,500	1.1×10^{-2}	Discrete protuberances

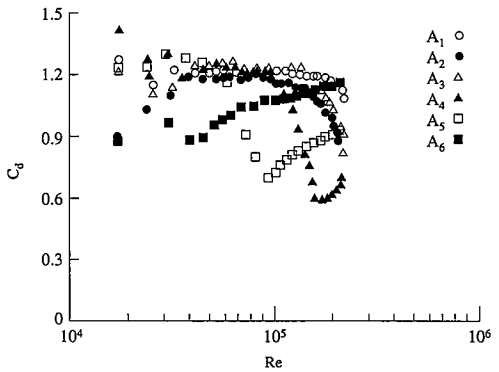

Fig.5 Relationship between drag coefficient and Reynolds number of Models A_1 - A_6

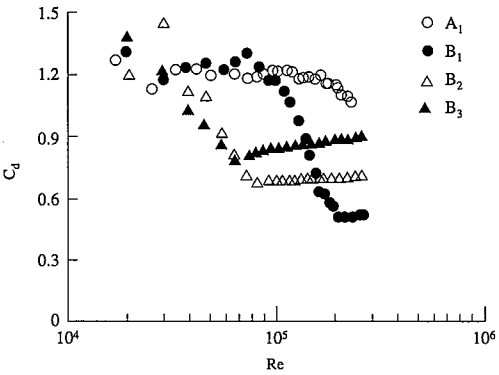

Fig.6 Relationship between drag coefficient and Reynolds number of Models B_1 - B_3

Fig.6 shows measurement results of the drag coefficients of Models B_1 - B_3, which have deformations of the same size as Models A_4 - A_6 but arranged in a grating pattern. Like Models A_4 - A_6 with evenly distributed surface deformations, the critical Reynolds numbers of the models having surface deformations in a grating pattern decreased as the deformations became larger, but their drag coefficients rose very slowly, somewhat in a different way from that of Models A. Model B_6, having surface deformations 1% of the diameter in size arranged in a grating pattern, showed a critical Reynolds number of about 7×10^4 and a drag coefficient C_d of about 1.0 at a Re of 2.2×10^5.

Fig.7 shows measurement results of drag coefficients of Models C_2 and C_3 wherein deformations in depressions and protuberances of about the same size as Models A_4 - A_6 were discretely arranged. Both of these models with deformations about 1% of the diameter in size showed roughly identical results: the drag coefficient C_d nearly equal to 0.6 at a critical Reynolds number of approximately 1×10^5. The measurement was continued up to a Reynolds number of 5.5×10^5 (tunnel wind speed roughly 55 m/s) and the drag coefficient did not show any tendency to rise in the wind speed band but stayed within a stable range.

As stated above, as have been pointed out in past reports, round section bodies show different peeling patterns of boundary layers on their surfaces depending on the shape and distribution of surface

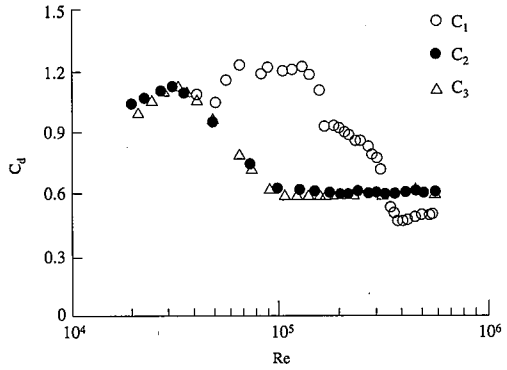

Fig.7 Relationship between drag coefficient and Reynolds number of Models C_1 - C_3

roughness as well as the size of the roughness, and their drag characteristics change in consequence. Through these tests it was observed that the drag coefficient decreased and the range of transition to turbulent flow peeling became wider as the percentage of smooth surface portions increased. Consequently, it was made clear that, by distributing the roughness discretely, the drag coefficient of a section with surface deformations could be lowered to a level close to that of a section without surface deformations even at the design wind speed, without changing the size of the deformations.

3.2 Static Aerodynamic Characteristics of Cables with Indented Surfaces

From the results of the fundamental tests, it was decided that the surface roughness should be in the form of oval depressions (indents) and the indents should be locally densely arranged in a pattern, leaving smooth indent-free surfaces. The roughness pattern used in these tests of the indented cable models[14] was chosen in consideration of ease of manufacturing and installation based on analyses of all the previous test results. **Fig.8** shows the surface pattern of Model D_2 as an example of the tested patterns used in the wind tunnel tests. No studies have yet been made to define the optimum combination pattern of the smooth and roughened portions to satisfy required conditions. Principal data of the models are listed in **Table 2**. These models were tested, like Models C, on the large circuit wind tunnel of Sumitomo Heavy Industries Ltd.

Whereas relative roughness (k/D) of the surface of common smooth cables is 0.002%, the same of the indented surface is 1%. Influence of a 1% surface roughness is not at all small: in case the entire cable surface is covered evenly with the indents, it is expected that the critical Reynolds number is reached at a relatively low wind speed with a drag coefficient of roughly 0.8 and, in the area near the

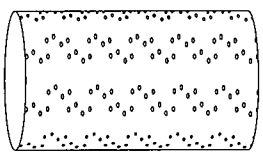

Fig.8 Model D_2 (Indented cable)

Table 2 Cable model data

Model	Diameter D (m)	Surface roughness k (μm)	Relative surface roughness (k/D)	Remarks
D_1	0.15	3	2.0×10^{-5}	Smooth surface
D_2	0.15	1,500	1.0×10^{-2}	Indented

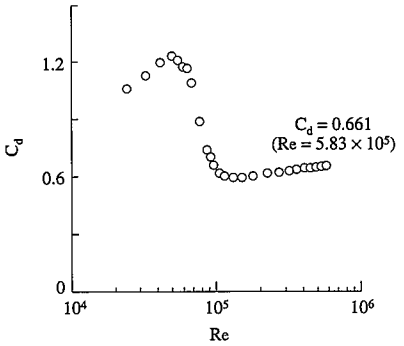

Fig.9 Relationship between drag coefficient and Reynolds number of Model D_2

design wind speed where the Reynolds number is higher, the drag coefficient will slightly rise to approximately 1. It had been expected that, in the case where the surface deformations were distributed unevenly like the indented models used in the tests, the physical relationship between airflow direction and the roughness pattern might influence the test results, but preliminary tests confirmed that such an influence was very small.

Fig.9 shows measurements of the drag coefficient and Reynolds number of the indented cable D_2. The maximum wind speed at the tests was 55 m/s, which corresponded to a Reynolds number of 5.5×10^5. The critical Reynolds number of the indented cable is approximately 1×10^5 and its drag coefficient is roughly 0.6. This drag coefficient value stays nearly constant in the range above the critical Reynolds number up to the maximum wind speed of the tests. Peripheral airflow of a columnar body usually fluctuates as Reynolds number changes, but the above drag coefficient nearly independent from the Reynolds number suggests that that is not occurring conspicuously. It was, therefore, made clear that the proposed surface indent pattern would not raise the drag coefficient to above 0.7 in the design wind speed range, making it possible to design the bridges in the same way as with smooth-surfaced cables.

4. Vibration Characteristics of Indented Cables

4.1 Rain Vibration Suppression Tests

A series of vibration tests were carried out[14] under conditions with and without rain for the purpose of studying rain vibration suppression characteristics of the surface-roughened cables. For avoiding deviation of the measured Reynolds number from the real one due to the use of scaled models, real size models were used. Principal data of the cable models and outline of the wind tunnel tests are shown in **Table 3** and **Fig.10**, respectively.

Cables 3 m long were used for vibration response measurements and they were supported so as to vibrate in right angles in a plain perpendicular to the cable axis. The mass of the model vibrating system was 7.8 kg/m, its natural frequency ranged from 0.45 to 1.25 Hz and logarithmic decrement under a no wind condition was approximately 0.003. Although the logarithmic decrement under a no wind condition was nearly identical to that of real cables, the models were susceptible to vibration, since the mass was only about 1/10 and

Table 3 Data of cable models for vibration tests

Model	Mass (kg/m)	Frequency (Hz)	Logarithmic decrement δ	Scruton number S_c
D_1	7.8	0.45 - 1.25	0.003	Approx. 2
D_2	7.8	0.45 - 1.25	0.003	Approx. 2

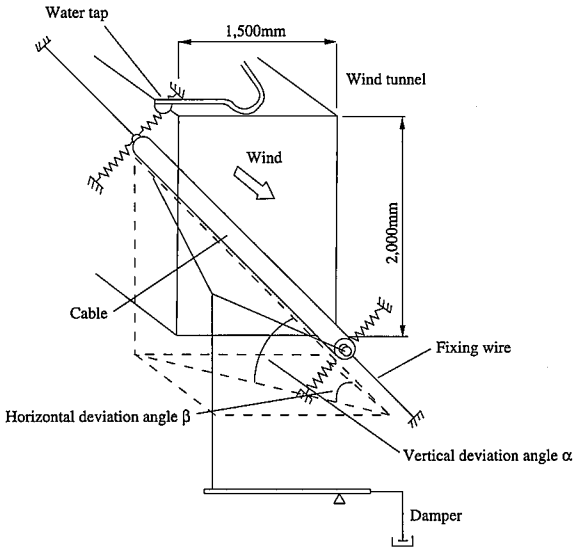

Fig.10 Outline of wind tunnel test

Scruton number S_C ($S_C = 2m\delta / \rho D^2$, where m is mass, and ρ is air density) was small. For this reason, the measurement of the vibration response of the cable model were compensated in consideration of Scruton number.

The cable posture was determined taking into consideration reports of frequent cable vibration cases and cable installation conditions in real long cable-stayed bridges, namely, the cable gradient in a vertical plain (α) was set at 20° and a deviation of the vertical plain from the wind axis (β) 45° for raining conditions, and α = 0° and β = 30° for non-raining conditions. Water was poured from above the cable model along its length for simulating rainfalls and the water quantity was set to a value that resulted in the largest vibration response at separate tests[15].

4.2 Vibration Suppression Effects

4.2.1 Vibration Response under Raining Conditions

Figs.11 and 12 show vibration responses (A/D, where A is amplitude and D is cable diameter) under the raining conditions of Model D_1 with a smooth surface and Model D_2 with an indented surface, respectively. A large divergent vibration, the so-called rain vibration, was observed with Model D_1 in a lower-order frequency of 0.45 Hz from a wind speed about 10 m/s It is also observed that there was a vibration response at a wind speed of about 5 m/s The divergent vibration occurring from about 10 m/s is nearly identical to that conventionally observed in a high frequency range. However, it is suspected that the vibration at about 5 m/s was caused by the low natural frequencies of long cables used in the latest long bridges. In the case of a frequency of 0.73 Hz, very large vibration was generated at wind speeds above 8 m/s, while vibration response was very small in the case of a frequency of 1.25 Hz.

With the indented Model D_2, there was a restricted vibration response of a frequency of 0.45 Hz at a low wind speed around 5 m/s although excitation was not strong. It is suspected that this vibration response occurs when the frequency is low and that it is frequency-dependent like in the cases of real cables. A large vibration suppression effect against the divergent vibration appears from 10 m/s or so, and in a frequency of 0.59 Hz or higher the vibration response is controlled very small. From the observation of water flow on the cable surface during the tests, formation of water flow routes on the cable surface seemed to be controlled, as envisaged, thanks to the

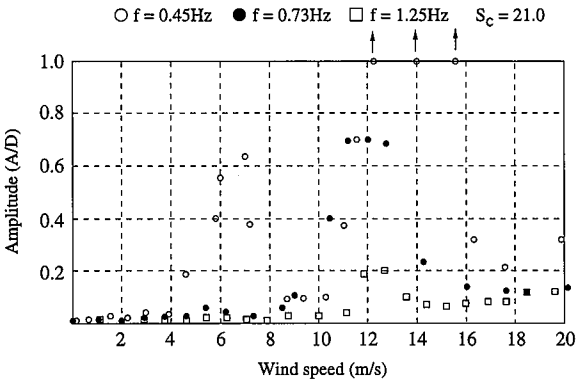

Fig.11 Vibration test results of Model D_1 (raining, in uniform airflow)

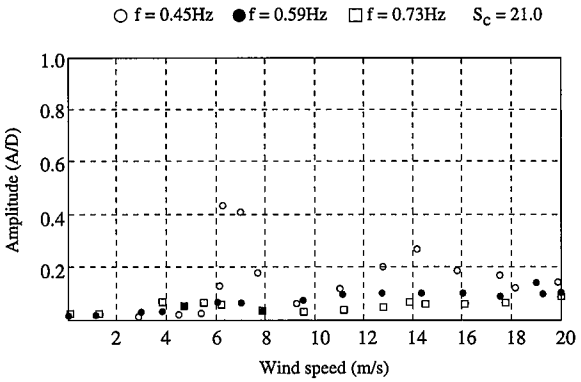

Fig.12 Vibration test results of Model D_2 (raining, in uniform airflow)

vibration restriction effects of the peripheral airflow brought about by the indented surface finishing.

Besides the above tests in a uniform airflow, another series of tests were carried out for observing changes of vibration characteristics in a turbulent flow. **Fig.13** shows results of tests under a turbulence intensity of approximately 10%. In the case where frequency is low, restricted amplitude vibration occurred to the indented cable in a low wind speed range in a uniform airflow. It was made clear however that, in a turbulent flow simulating the situations of real bridges, the amplitude of the low frequency vibration became very small - less than a half of that in the uniform flow.

Besides the above, in real bridges the indents on the upper side of cables are filled with dust and made flat during the service life. This situation was also tested and it was confirmed that the vibration sup-

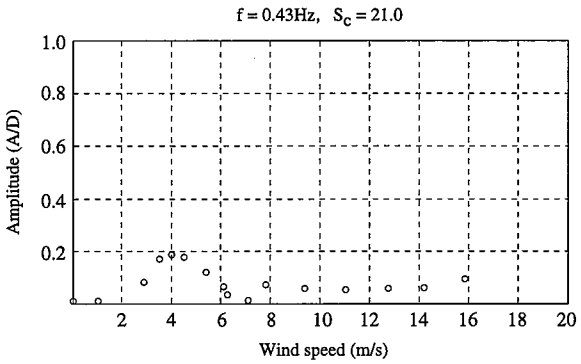

Fig.13 Vibration test results of Model D_2 (raining, in turbulent airflow)

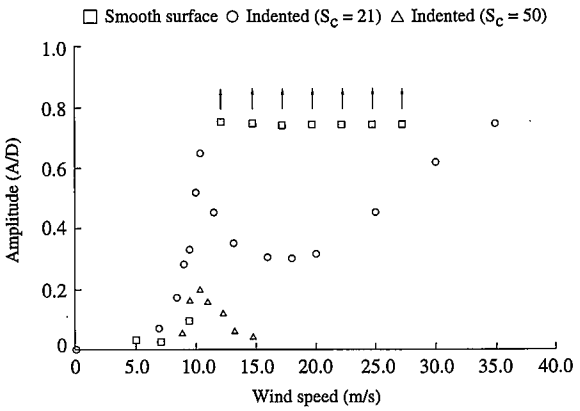

Fig.14 Vibration test results of Model D_2 (not raining, in uniform airflow)

pression effects were not affected even if the indents on the upper side were made flat with dust.

4.2.2 Vibration Response under No-rain Conditions

Tests were carried out also under no-rain conditions in consideration of the views maintaining that a two-dimensional inclined columnar body is prone to aerodynamic vibration due to existence of airflow along the axis of the body. **Fig.14** shows vibration responses of the indented cable model D_2 used as a slanted column. As it was said that such a vibration response would occur in a comparatively high wind speed range, the observation was done in a range of a reduced wind velocity (f·D/U) of approximately 400. The vibration response began to show from 10 m/s and the vibration developed gradually as the wind speed increased. Divergent vibration began to appear with the indented cable at a wind speed of 30 m/s, higher than with the smooth-surfaced cable D_1. In a range where the Scruton number was about 50, amplitude of restricted vibration was small enough although the vibration responses persisted. These tests were done in a uniform airflow only and influence of turbulent airflow was not studied, but it is commonly considered that the response in a turbulent airflow does not surpass the same in a uniform airflow.

4.3 Pressure Distribution Characteristics

Cables with discretely distributed indents show static characteristics and rain vibration suppressing behavior markedly different from those with a smooth surface. The properties of the former were analyzed through studies of their pressure distribution characteristics. Pressure measurement was done by sequentially scanning 36 pressure holes drilled along the cable circumference at 10° intervals.

Figs.15 and 16 show average pressure coefficients C_p at the surface. With the original smooth-surfaced cable model D_1, a pressure drop on the lateral sides and a pressure recovery in the airflow peeling region on the downstream side are seen to occur gradually as the Reynolds number increases. This fact indicates that the state of airflow is gradually changing as Reynolds number changes. On the other hand, with the indented cable D_2, a nearly constant pressure distribution is maintained in the Reynolds number range above the critical Reynolds number (0.9×10^5) regardless of the wind speed, and its pressure distribution pattern is roughly identical to that of the smooth-surfaced cable in the high Reynolds number range (5.5×10^5). From the fact that the drag coefficient of the indented cable is slightly over 0.6 in the corresponding Reynolds number range, it is presumed that a constant peripheral flow is formed by the indented surface in the range above the critical Reynolds number.

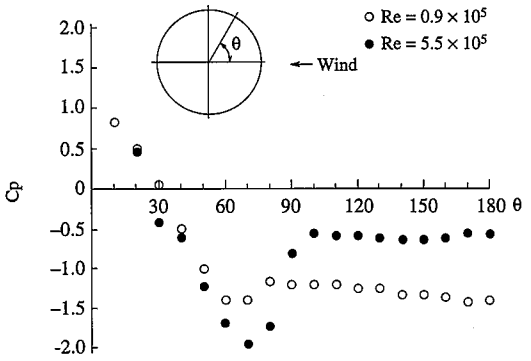

Fig.15 Pressure distribution measurement of Model D_1

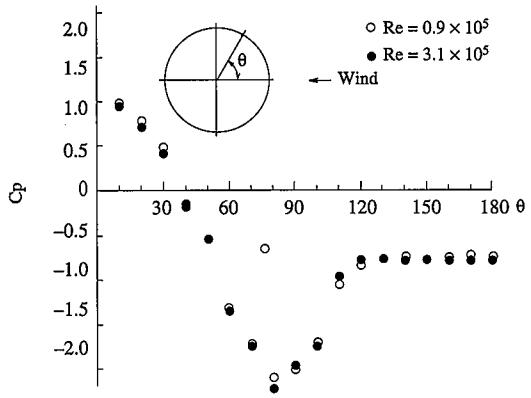

Fig.16 Pressure distribution measurement of Model D_2

5. Manufacture of Vibration Suppressing Cables

5.1 Application to the Tatara Bridge

The Tatara Bridge is a cable-stayed bridge between Ikuchijima Island and Omishima Island along the Onomichi-Imabari Route of the Honshu-Shikoku Bridge Links. It is the longest cable-stayed bridge in the world with a total length of 1,480 m and a center span of 890 m, longer by 34 m than the Normandy Bridge. (See **Fig.17**.) It has a 3-span continuous compound box girder of steel and PC, since its side spans are short in proportion to the center span and, for balancing the dead weight, PC girders are used at an end of each of the side spans. The cable arrangement is of a 2-plain 21-stage multi-fan type and coated parallel strands are used for the cables.

In proportion to the bridge length, the cables of the Tatara Bridge are also long: the longest one is about 460 m long and its lowest order frequency of 0.26 Hz is far lower than that of any bridges built previously and, therefore, measures were indispensable for suppressing cable vibration. As a result of studies on the rain vibration control measures[16], it was made clear that, for obtaining sufficient vibration restriction effects by installation of dampers, they had to be installed at very high positions (about 4.5 m above the girder), and various problems were expected in relation to the equipment and structure. A basic policy was therefore agreed to the effect that aero-

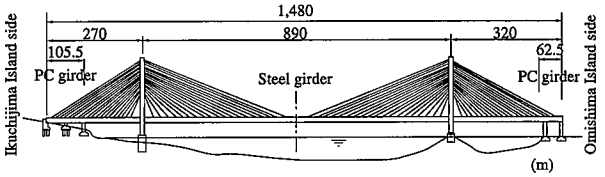

Fig.17 General elevation view of the Tatara Bridge

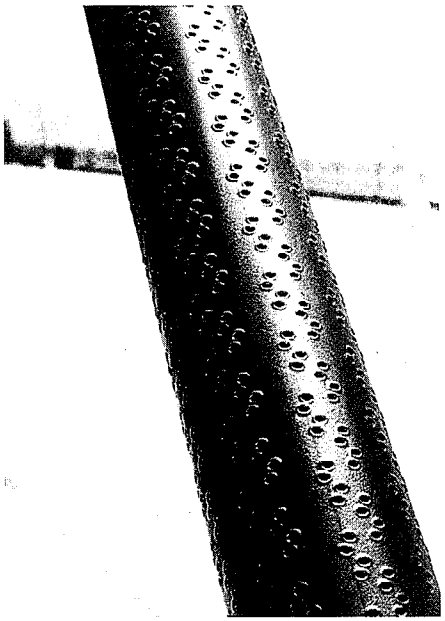

Photo 2 Indented cable of the Tatara Bridge

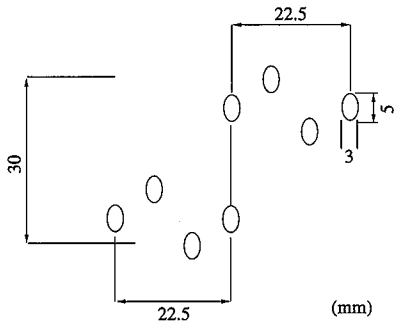

Fig.18 Indent pattern

dynamic measures should be employed in order to enhance intrinsic wind stability of the cables. In the design of the Tatara Bridge the drag coefficient C_d of the cables was set at 0.7 and, in consideration of the results of the previous studies, indented-surface cables[17] offering a low drag and a high vibration suppression effect were selected. (See **Photo 2**.)

5.2 Manufacturing of the Cables

The cables are made of 7 mm diameter galvanized steel wires having a tensile strength of 160 kgf/mm² (1,570 N/mm²), formed into strands with slight twisting and then coated with extruded high density polyethylene (NEW-PWS). Nippon Steel supplied about 2,000 t of the cables for the center span. Their lengths range from 110 to 460 m and the outer diameters from 110 to 170 mm. The indents were formed after the cables were coated with the extruded polyethylene. **Fig.18** shows details of the indent pattern.

6. Conclusions

As cable-stayed bridges become longer to attain a 1,000-m class total length, importance increases of aerodynamic measures for enhancing wind stability of the cables for suppressing their vibration. This report describes s newly developed indented cable as an aerodynamic measure suitable for particular requirements of the cables for long cable-stayed bridges.

The indented cable has a patterned roughness on its surface wherein smooth portions and portions where deformations are densely arranged are combined. This type of cable is effective for restricting rain vibration since it maintains a drag coefficient in the design wind velocity range as low as a smooth-surfaced cable. The solution proposed in the present study is to control peripheral airflow around a columnar body by a patterned roughness on the surface of the body. This method is considered applicable not only to suppressing cable vibration in long cable-stayed bridges but also to any cylindrical structures, and the authors intend to further develop its application technologies.

The vibration suppression cable described herein was applied to the Tatara Bridge and its effectiveness in the real scale has been confirmed as no rain vibration has been reported[18] in cable vibration observations for a year after the completion of the bridge construction.

Acknowledgement

The authors should like to thank Profs. Miyata and Yamada of the Yokohama National University and related people of Honshu-Shikoku Bridge Authority and the Joint Venture for Tatara Bridge Construction for their collaboration in the studies of wind resistibility and vibration suppression measures of the cables. Thanks are also extended to the people of Sumitomo Heavy Industries Ltd. for their cooperation in relation to the wind tunnel tests.

Reference

1) National Land Development Technology Research Center: Report on Study of Wind Resistance of Cables in Cable-stayed Bridges. 1989
2) Public Work Research Center: Study Report on Wind Resistibility of Cables for Cable-stayed Bridges. 1993
3) Hikami, Y.: Rain Vibration of Cable-stayed Bridge Cables. Proc. Jpn. Ass. Wind Eng. 27, 17-28 (1986)
4) Okauchi, Ito, Miyata: Wind-resistant Structure. Maruzen, 1977
5) Matsumoto, et al.: Study on Main Two Causes of Rain Vibration in Cable-stayed Bridges. Proc. 11th Wind Eng. Symp. 1990
6) Yokoyama, Kusakabe: Wind-induced Vibration of Cables in Cable-stayed Bridges and Its Countermeasures. Bridge & Foundation Engineering. 74-84 (1989-8)
7) Yoneda: Wind-induced Vibration of Cables in Cable-stayed Bridges. 2nd Colloquium on Vibration Control, Part A. 1993-8
8) Matsumoto, M., Hikami, Y., Kitazawa, M.: Cable Vibration and Its Aerodynamic/Mechanical Control, Cable-stayed and Suspension Bridge. Deauville, France, Oct. 1994
9) Matsumoto, M., et al: Wind-resistant Design of the Higashi-Kobe Bridge. Bridges & Foundations Engineering, 35-43 (1991-5)
10) Miyazaki, Saito, Suzuki: Aerodynamic Vibration Measures of Cables in Cable-stayed Bridges. Proc. 48th Annual Meeting of JSCE. 1993
11) Flamond, O.: Rain-wind Induced Vibration of Cables, Cable-stayed and Suspension Bridge. Deauville, 1994-10
12) Miyata, Y., Yamada, H., Hojo, T.: Experimental Study on Aerodynamic Characteristics of Cables with Patterned Surface. Bridges & Foundations Engineering. 30-36 (1993-9)
13) Miyata, Y., Yamada, H., Hojo, T.: Experimental Study on Aerodynamic Characteristics of Cables with Patterned Surface. Journal of Structural Engineering. 40A, 1065-1076 (1994)
14) Hojo, T., Yamazaki, Miyata, T., Yamada, H.: Development of Aerodynamically Stable Cables for Cable-stayed Bridges Having Low Resistance. Bridges & Foundations Engineering, 27-32 (1995-6)
15) Hojo, T.: Experimental Study on Rain Vibration Characteristics of Cables for Cable-stayed Bridges and Anti-vibration Measures. Proc. Jpn. Ass. Wind Eng. 50, 19-26 (1992)
16) Fujiwara, T., Moriyama, A.: Vibration Control of Cables of the Tatara Bridge., Honshu-Shikoku Bridge Authority Technical Report. 31-41 (1996-7)
17) Miyata, T., Yamada, H., Fujiwara, T., Hojo, T.: Wind-resistant Design of Cables for the Tatara Bridge. IABSE Symposium, Kobe, 1998
18) Fujiwara, T., Moriyama, A., Manabe: Measures against Cable Vibration for the Tatara Bridge. Bridges & Foundations Engineering, 16-19 (1999-5)